The Astrophysical Journal Letters, 809:L27 (6pp), 2015 August 20 doi:10.1088/2041-8205/809/2/L27

DISCOVERY OF A HIGHLY POLARIZED OPTICAL MICROFLARE IN BLAZAR S5 0716+714 DURING THE 2014 WEBT CAMPAIGN*

G. Bhatta[1], A. Goyal[1], M. Ostrowski[1], Ł. Stawarz[1], H. Akitaya[2], A. A. Arkharov[3], R. Bachev[4], E. Benítez[5], G. A. Borman[6], D. Carosati[7,8], A. D. Cason[28], G. Damljanovic[9], S. Dhalla[10], A. Frasca[11], S-M. Hu[12], R. Itoh[13], S. Jorstad[14,15], D. Jableka[1], K. S. Kawabata[2], S. A. Klimanov[3], O. Kurtanidze[16,17,18], V. M. Larionov[3,15], D. Laurence[10], G. Leto[11], A. Markowitz[19], A. P. Marscher[14], J. W. Moody[20], Y. Moritani[21], J. M. Ohlert[22], A. Di Paola[23], C. M. Raiteri[24], N. Rizzi[25], A. C. Sadun[26], M. Sasada[14], S. Sergeev[6], A. Strigachev[4], K. Takaki[13], I. S. Troitsky[15], T. Ui[13], M. Villata[24], O. Vince[9], J. R. Webb[10], M. Yoshida[2], S. Zola[1,27], and D. Hiriart[28]

[1] Astronomical Observatory of Jagiellonian University, ul. Orla 171, 30-244 Krakow, Poland; gopalbhatta716@gmail.com
[2] Hiroshima Astrophysical Science Center, Hiroshima University, Higashi-Hiroshima, Hiroshima 739-8526, Japan
[3] Main (Pulkovo) Astronomical Observatory of RAS, Pulkovskoye shosse, 60, 196140 St. Petersburg, Russia
[4] Institute of Astronomy, Bulgarian Academy of Sciences, 72, Tsarigradsko Shosse Boulevard, 1784 Sofia, Bulgaria
[5] Instituto de Astronomía, Universidad Nacional Autónoma de México, Mexico DF, Mexico
[6] Crimean Astrophysical Observatory, P/O Nauchny, Crimea 298409, Russia†
[7] EPT Observatories, Tijarafe, La Palma, Spain
[8] INAF, TNG Fundacion Galileo Galilei, La Palma, Spain
[9] Astronomical Observatory, Volgina 7, 11060 Belgrade, Serbia
[10] Florida International University, Miami, FL 33199, USA
[11] Osservatorio Astrofisico di Catania, Italy
[12] Shandong Provincial Key Laboratory of Optical Astronomy and Solar-Terrestrial Environment, Institute of Space Sciences, Shandong University at Weihai, 264209 Weihai, China
[13] Department of Physical Science, Hiroshima University, Higashi-Hiroshima, Hiroshima 739-8526, Japan
[14] Institute for Astrophysical Research, Boston University, 725 Commonwealth Avenue, Boston, MA 02215, USA
[15] Astronomical Institute, St. Petersburg State University, Universitetskij Pr. 28, Petrodvorets, 198504 St. Petersburg, Russia
[16] Abastumani Observatory, Mt. Kanobili, Abastumani, Georgia
[17] Engelhardt Astronomical Observatory, Kazan Federal University, Tatarstan, Russia
[18] Landessternwarte Heidelberg-Konigstuhl, Germany
[19] University of California San Diego, 9500 Gilman Drive, La Jolla, CA 92093, USA
[20] Physics and Astronomy Department, Brigham Young University, N283 ESC, Provo, UT 84602, USA
[21] Kavli Institute for the Physics and Mathematics of the Universe (KavliI PMU), The University of Tokyo, 5-1-5 Kashiwa-no-Ha, Kashiwa City, Chiba 277-8583, Japan
[22] Astronomie Stiftung Tebur, Fichtenstrasse 7, D-65468 Trebur, Germany
[23] INAF—Osservatorio Astronomico di Roma, via Frascati 33, I-00040 Monte Porzio, Italy
[24] INAF—Osservatorio Astronomico di Torino, Italy
[25] Sirio Astronomical Observatory Castellana Grotte (Ba), Italy
[26] Department of Physics, University of Colorado Denver, Denver, CO, USA
[27] Mt. Suhora Observatory, Pedagogical University, ul. Podchorazych 2, 30-084 Krakow, Poland
[28] Instituto de Astronomía, Universidad Nacional Autónoma de México, Ensenada, Mexico
Received 2015 July 13; accepted 2015 July 28; published 2015 August 18

ABSTRACT

The occurrence of low-amplitude flux variations in blazars on hourly timescales, commonly known as microvariability, is still a widely debated subject in high-energy astrophysics. Several competing scenarios have been proposed to explain such occurrences, including various jet plasma instabilities leading to the formation of shocks, magnetic reconnection sites, and turbulence. In this Letter, we present the results of our detailed investigation of a prominent, five-hour-long optical microflare detected during the recent WEBT campaign on 2014 March 2–6 targeting the blazar 0716+714. After separating the flaring component from the underlying base emission continuum of the blazar, we find that the microflare is highly polarized, with the polarization degree $\sim$(40–60)% $\pm$ (2–10)% and the electric vector position angle $\sim$(10–20)° $\pm$ (1–8)° slightly misaligned with respect to the position angle of the radio jet. The microflare evolution in the (Q,U) Stokes parameter space exhibits a looping behavior with a counterclockwise rotation, meaning the polarization degree decreases with the flux (but is higher in the flux decaying phase), and an approximately stable polarization angle. The overall very high polarization degree of the flare, its symmetric flux rise and decay profiles, and also its structured evolution in the $Q-U$ plane all imply that the observed flux variation corresponds to a single emission region characterized by a highly ordered magnetic field. As discussed in the paper, a small-scale but strong shock propagating within the outflow, and compressing a disordered magnetic field component, provides a natural, though not unique, interpretation of our findings.

* The data collected by the WEBT Collaboration are stored in the WEBT archive; for questions regarding their availability, please contact the WEBT President Massimo Villata (villata@oato.inaf.it).
[29] Private address: 105 Glen Pine Trail, Dawnsonville, GA 30534, USA.
† While the AAS journals adhere to and respect UN resolutions regarding the designations of territories (available at http://www.un.org/press/en), it is our policy to use the affiliations provided by our authors on published articles.

Key words: acceleration of particles – BL Lacertae objects: individual (S5 0716+714) – galaxies: active – galaxies: jets – polarization – radiation mechanisms: non-thermal

1. INTRODUCTION

Blazars are known for their intense non-thermal emission and pronounced variability across the electromagnetic spectrum, resulting from the efficient energy dissipation taking place in the innermost regions of relativistic, magnetized, and non-stationary outflows—"jets"—produced by active supermassive black holes in the centers of the evolved galaxies (e.g., Begelman et al. 1984; Meier 2012). However, our understanding of the exact physical conditions of the emitting plasma in blazar jets remains limited. The occurrence of rapid and low-amplitude flux variations on hourly timescales, commonly known as microvariability, or intra-day/night variability (e.g., Wagner & Witzel 1995 and references therein), provides additional challenges in this context, as the amount of relativistic beaming required by the plausible explanation for such phenomena is, in many cases, too extreme to be reconciled with the currently favored models for the jet formation in active galactic nuclei (AGNs).

Several competing scenarios have been proposed to explain rapid, low- or high-amplitude variability in blazar sources. Some include *extrinsic causes*, such as gravitational microlensing (Watson et al. 1999; Webb et al. 2000); others involve *intrinsic origin*, including purely geometrical effects (e.g., the "light house effect"; Camenzind & Krockenberger 1992), or various plasma instabilities leading to the formation of shocks, magnetic reconnection sites, and turbulence (see the recent discussions in, e.g., Narayan & Piran 2012; Subramanian et al. 2012; Marscher 2014; Saito et al. 2015; Sironi et al. 2015). Since the radio-to-optical emission continuum of blazars (and BL Lacertae objects in particular) is known to be due to the synchrotron radiation by ultrarelativistic jet electrons, the temporal behavior of the optical polarization can be used as a powerful tool for diagnosing the structure of the blazar emission zone and the source of their variability.

For example, a significant polarization degree of the synchrotron flux indicates an anisotropic distribution of the jet magnetic field, which may be related to either a large-scale uniformity of the magnetic field lines (e.g., Begelman et al. 1984; Lyutikov et al. 2005) or a tangled, chaotic magnetic field compressed or sheared by the flow (e.g., Laing 1980, 2002; Hughes et al. 1985; Cawthorne & Cobb 1990; Kollgaard et al. 1990; Wardle et al. 1994; Nalewajko 2009). Moreover, the high duty cycle of the blazar *polarization* microvariability revealed by multi-frequency optical monitoring ($\gtrsim$50%; e.g., Andruchow et al. 2005; Villforth et al. 2009) indicates an origin linked to changes in the physical conditions of the jet plasma, rather than some external (to the jet) or purely geometrical effects.

In this Letter, we present the results of our detailed investigation of a particularly prominent and well-resolved optical microflare detected during the Whole Earth Blazar Telescope (WEBT[30]) campaign targeting S5 0716+714 on 2014 March 2–6. During the campaign, high-quality, simultaneous multi-band optical flux and polarization measurements of the source have been gathered. S5 0716+714 is one of the brightest blazars of the "intermediate-frequency-peaked BL Lac object" type, exhibiting persistent activity in all wavebands, including radio, optical, and γ-rays (e.g., Bhatta et al. 2013; Rani et al. 2015). In particular, the source is known to show rapid optical fluctuations on timescales of minutes and hours (Fan et al. 2011; Bhatta et al. 2013; Wu et al. 2014); high and variable optical polarization degrees of about $\gtrsim$30%, along with fast rotations of the position angle of the electric vector, also have been observed (e.g., Larionov et al. 2013). The microvariability duty cycle of S5 0716+714 is very high ($\sim$80%–90%; Webb 2007; Hu et al. 2014) when compared with that of other blazars or other types of AGNs (see Goyal et al. 2013). The selected source is therefore an ideal target for studying polarization and spectra properties of the blazar optical microvariability. Below, we discuss the detection of the very high polarization degree of the microflare component separated from the underlying, slowly varying emission continuum in S5 0716+714, indicating a highly ordered magnetic field in the sub-region of the jet responsible for the production of the observed flux enhancement.

2. THE 2014 WEBT CAMPAIGN

The simultaneous photo-polarimetric observations of S5 0716+714 analyzed here were obtained as a part of the WEBT campaign that lasted for five days, 2014 March 2–6. At that time, the source was in a low activity-level state, slowly increasing its optical flux after the historical minimum from the end of 2013. The gathered data set consists of high-quality, high-cadence multi-channel (BVRI) flux measurements from several observatories; on two occasions, lasting for about 20 hr (56719.44–56720.27 MJD; hereafter "Epoch 1") and 18 hr (56721.70–56722.44 MJD; "Epoch 2"), the high-quality optical polarimetric observations were obtained from St. Petersburg (LX-200), Crimea (AZT-8), Flagstaff, AZ (1.8 m Perkins), and Kanata (1.5 m) telescopes. Detailed analysis of the entire data set collected during the 2014 WEBT campaign, along with the discussion on data acquisition and reduction, will be presented elsewhere (G. Bhatta et al. 2015, in preparation).

3. ANALYSIS AND MODELING RESULTS

Figure 1 presents the photo-polarimetric data set gathered in the R band for Epoch 2 of the 2014 WEBT campaign targeting S5 0716+714; the flux measurements in the remaining filters are more sparse, especially in the B-band during the epoch considered. As shown, a very prominent and well-resolved microflare with the approximately symmetric and almost exponential flux rise and decay profiles—and a sharp peak in between—was observed in the period 79–85 hr (from the campaign starting time at 0 hr; see the dashed vertical lines in the figure). The total observed intensity of the source varied at that time by $\sim$10% in $\tau_{\rm var} \simeq 2$ hr. In order to extract the main characteristics of the flaring component, first, we define the polarization degree *PD*, the position angle of the electric vector χ, and the polarized flux *PF* through the Stokes parameters *Q*

[30] http://www.to.astro.it/blazars/webt/

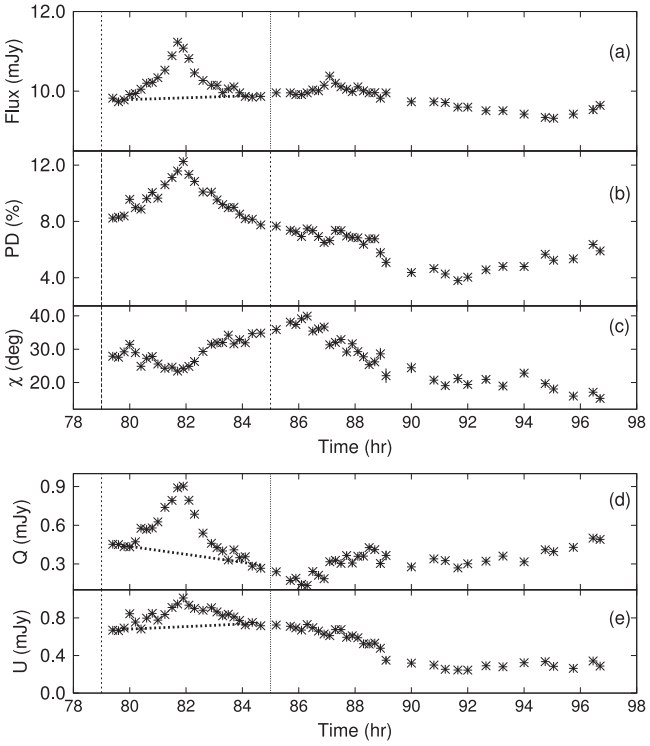

Figure 1. Photo-polarimetric optical data collected for the blazar S5 0716+71 during Epoch 2 of the 2014 WEBT campaign. Subsequent panels from top to bottom present the total observed R-band flux F, the corresponding total polarization degree PD, the position angle of the electric vector χ, and the Stokes parameters Q and U. The dashed lines in panels (a) and (d)–(e) denote the modeled "background" emission continuum. The period analyzed in this Letter is marked by the two vertical dashed lines (between 79 and 85 hr after the start of the campaign).

and U (see Rybicki & Lightman 1986):

$$PD = \frac{\sqrt{Q^2 + U^2}}{F},$$
$$\chi = \frac{1}{2}\tan^{-1}\left(\frac{U}{Q}\right), \quad \text{and}$$
$$PF = \sqrt{Q^2 + U^2}, \tag{1}$$

where F is the total flux of the source.

Next, we assume that the analyzed microflare constitutes a separate emission component superimposed on the underlying, slowly variable "background" provided by the base emission continuum of the blazar. Due to the linearly additive properties of total flux and the Stokes Q and U intensities, one therefore has

$$F = F_0 + F_1,$$
$$Q = Q_0 + Q_1, \quad \text{and}$$
$$U = U_0 + U_1, \tag{2}$$

where the microflare and the base emission components have been denoted by indices "1" and "0," respectively. In the modeling of this particular microflare, all the background intensities (F_0, Q_0, and U_0) are found from fitting the data collected just before (79–80 hr) and just after (84–85 hr) the microflare, assuming that these may change slowly (linearly) with time (see the dashed lines in the corresponding panels of Figure 1). Once the base intensities are found, we subtract them

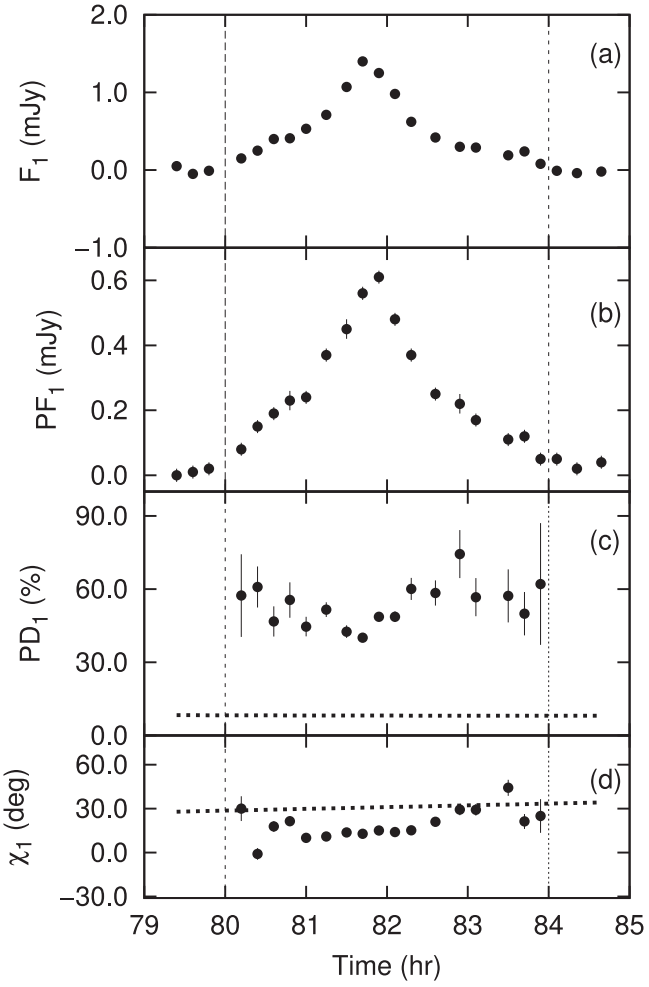

Figure 2. Derived basic parameters of the flaring component in S5 0716+71. Subsequent panels from top to bottom present the R-band flux F_1, the corresponding polarized flux PF_1, the total polarization degree PD_1, and the position angle of the electric vector χ_1. Dashed lines in the panels (c) and (d) denote the modeled "background" emission continuum. The duration of the microflare is marked by the two vertical dashed lines.

from the total intensities, to obtain F_1, Q_1, and U_1, which further enable us to derive the basic parameters for the flaring component, PD_1, χ_1, and PF_1, using the standard relations given in Equation (1).

In the above analysis, we use the data exclusively in the R filter, for which continuous flux measurements are available in both the intensity and polarization for the entire duration of Epoch 2. To derive the errors for the base intensities, we take the square root of the average of the variances of the data points used for the background component fitting (i.e., just before and after the microflare). This is indeed a reasonable assumption since in the absence of a flaring component (which increases the signal-to-noise ratio, thereby reducing the measurement uncertainty; see Howell 1989), the errors of the flux measurement should correspond to those of the slowly varying background continuum. The errors in the derived quantities (PD, χ, and PF), for both the base and the microflare emissions components, are derived using the standard error propagation formulae (Bevington & Robinson 2003).

Thus, derived basic parameters of the flaring component in S5 0716+71 are presented in Figure 2. As shown, the microflare is highly polarized, with $PD_1 \sim (40\text{–}60)\% \pm$

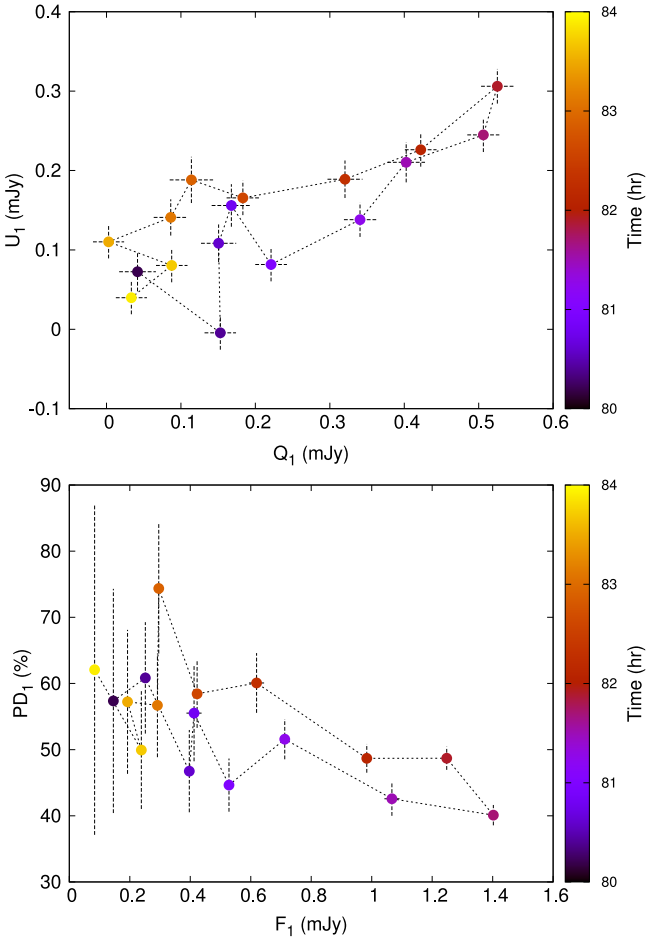

Figure 3. Evolution of the analyzed microflare in S5 0716+71 in the Stokes parameter plane Q_1 vs. U_1 (upper panel) and in the F_1–PD_1 plane (lower panel).

(2–10)%, especially when compared with the slowly varying base emission for which $PD_0 \sim 8\% \pm 0.01\%$. Interestingly, the electric vector position angle of the flaring component, $\chi_1 \sim (10\text{–}20)^\circ \pm (1\text{–}8)^\circ$, is only slightly different from that characterizing the underlying background component, $\chi_0 \sim 30^\circ \pm 0.8^\circ$. It is important to note that, according to the high-resolution radio image obtained on 2014 February 24 within the VLBA-BU-BLAZAR[31] project, χ_0 is close to the innermost (within 0.12 mas from the core) position angle of the jet ($\sim$45°), while χ_1 corresponds to the position angle of the jet farther down from the core ($\sim$20°).

In Figure 3, we also present the evolution of the flaring event in the Stokes parameter plane Q_1 versus U_1 (upper panel). As shown, there is an indication for a looping behavior with a counterclockwise rotation, i.e., with a higher polarization degree occurring in the decaying phase of the microflare. In general, the $Q-U$ diagrams illustrate the evolution of the polarized flux *together* with that of the polarization angle. In the particular case presented here, the observed behavior therefore implies a consistent rate of PF_1 changes (given by the distance between the consecutive data points), with no significant rotation of χ_1. This is a very interesting result, as some of the similar studies on optical variability show "random walk"-type behavior in the $Q-U$ plane; whereas only a few cases reveal a structured evolution (e.g., Uemura et al. 2010 and references therein). Moreover, during the analyzed microflare, the polarization degree of the flaring component *decreases* with the flux: as shown in the lower panel of Figure 3, even though the uncertainties in the polarized flux measurements are large in the beginning and at the end when the flaring component nearly equals the baseline emission, there is a clear counterclockwise looping in the PF_1 versus F_1 plane, with the polarization degree reaching a minimum at the level of $\sim$40% at the peak of the flare. We will come back to this interesting finding in Section 4.

Finally, we attempt a limited spectral analysis for the microflare, using the available BVRI data and considering the multi-band flux measurements to be simultaneous if collected within 10 minute windows. After separating the base components of the microflare in all the filters, we evaluate the spectral indices of the base component before and after the microflare, assuming a power-law distribution of $F_\nu \propto \nu^{-\alpha}$. In this way, we find that the spectral shape of the base emission continuum is nearly constant in time (for the period analyzed), with $\alpha_0 \simeq 1.44 \pm 0.01$. Next, we estimate the spectral index for the flaring component from the residual (total minus base) multi-band fluxes. Rather sparse BVI data, however, allow us to estimate only roughly the spectral slopes of the flaring component in the initial and final phases of the flux enhancement. The resulting spectral indices vary between $\alpha_1 \sim 1.15 \pm 0.07$ and $\sim 1.46 \pm 0.16$; large uncertainties, however, preclude us from making any definitive statements on the spectral evolution of the flaring component.

4. DISCUSSION

A few studies exist in the literature where attempts have been made to separate a base emission component from a variable emission component in the total and polarized flux optical observations of blazars. In most cases, the authors assumed a constant background and derived relatively high values for the polarization degree of flaring components ($\sim$20%–50%), with the electric vector position angles typically aligned to the jet directions (Hagen-Thorn et al. 2008; Sakimoto et al. 2013; Morozova et al. 2014; Covino et al. 2015). Particularly interesting for the work presented here are the results reported by Sasada et al. (2008) for S5 0716+714 based on the photo-polarimetric Kanata data gathered on 2007 October 20; these authors allowed for slow (linear) changes in the base emission continuum, deriving for the variable component, $PD \approx 27\%$, with $\chi \approx 150^\circ$ basically constant during the flaring event. For the flare analyzed in this Letter, we found a much higher polarization degree of $\sim$40%–60%, and the polarization angle $\sim$10°–25° was only slightly misaligned (by $\lesssim$20°, at most) with respect to the polarization angle of the base component, or to the position angle of the mas-scale radio jet.

The observed high polarization degree of the flare, its symmetric flux rise and decay profiles, and also its structured evolution in the $Q-U$ plane, all imply that the observed flux variation corresponds to a single and well-defined emission region characterized by a highly ordered magnetic field. A small-scale but strong shock wave propagating within the outflow, and efficiently compressing a disordered small-scale jet magnetic field component, is a natural and often invoked interpretation. In fact, the stable electric polarization angle positioned along the jet axis can easily be reconciled with the

[31] https://www.bu.edu/blazars/VLBA_GLAST/0716.html/

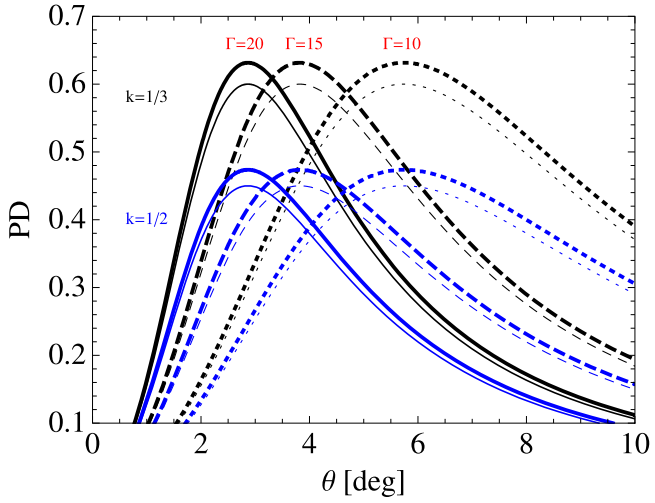

Figure 4. Expected polarization degree *PD* from a compression at the front of a strong shock as a function of the angle between the shock normal and the line of sight θ, calculated using Equation (3) for three values of the bulk Lorentz factor $\Gamma = 10$, 15, and 20 (dotted, dashed, and solid curves, respectively) with $\alpha = 1.5$ and 1.0 (thick and thin curves, respectively), and $k = 1/3$ and $1/2$ (black and blue curves, respectively).

shock interpretation. Moreover, in the case of a propagating shock, one may naturally expect a counterclockwise looping behavior in the $F-PD$ plane with the polarization degree correlated with the flux, resulting from the increasing shock compression in the initial phase, followed by the decompression and spectral steepening due to radiative cooling of the emitting particles at the later stages of the shock evolution (e.g., Hagen-Thorn et al. 2008; see also in this context the discussion in Perlman et al. 2011 regarding the optical polarimetric data for the flaring HST-1 knot in the M87 jet). In the case of the data set analyzed here, we do observe the counterclockwise looping, however, with the polarization degree *anti-correlated* with the flux.

In order to discuss this finding in more detail, though still only qualitatively, let us first note that the polarization degree expected from a shock compression can be expressed as

$$PD = \frac{3+3\alpha}{5+3\alpha}\,\frac{\delta^2\left(1-k^2\right)\sin^2\theta}{2-\delta^2\left(1-k^2\right)\sin^2\theta}, \qquad (3)$$

where α is the spectral slope of the non-thermal emission continuum, $1/k$ is the shock compression ratio, and $\delta = 1/\Gamma\,(1-\beta\cos\theta)$ is the Doppler factor of the emitting plasma characterized by the bulk Lorentz factor $\Gamma = (1-\beta^2)^{-1/2}$ and the angle between the shock normal and the line of sight θ (e.g., Kollgaard et al. 1990). Here, we evaluate polarization degree as a function of θ for a number of parameters relevant to our study. Following our spectral analysis presented at the end of Section 3, we chose the two limiting values of the spectral index $\alpha = 1.0$ and 1.5 and set $k = 1/3$ as appropriate for a strong and relativistic (in the jet rest-frame) shock; we also consider weaker shocks with $k = 1/2$ for comparison. We then take the three representative values of $\Gamma = 10$, 15, and 20, with the limitation of $\theta \leqslant 10^\circ$, for illustrative purposes only, noting that the analysis and modeling of the radio interferometric data regarding structural changes in the mas-scale jet of S5 0716+71 implies the jet viewing angle $\theta_j \lesssim 5^\circ$ and the jet Doppler factor $10 < \delta_j < 30$ (e.g., Bach et al. 2005; Rani et al. 2015 and references therein).

With the given free parameters, we find that the expected value of the polarization degree depends strongly on the combination of Γ and θ. As illustrated in Figure 4, even small changes in both parameters may result in significant changes in *PD*, whereas the change in α by 0.5 may not produce an appreciable change in *PD*. This exercise suggests in particular that the observed counterclockwise looping behavior with the polarization degree anti-correlated with the flux could possibly be explained by assuming that at the initial stages of the shock evolution the shock normal starts to deviate from the jet axis (in a sense, $\theta > \theta_j$) and that after the peak of the flare the disturbance decelerates, finally aligning its direction to that of the large-scale outflow. Interestingly, a careful look at the χ_1 evolution in the bottom panel of Figure 2 suggests that such a scenario may indeed be the case. Also, the maximum polarization degree expected in the model for the *maximum* shock compression corresponding to $k = 1/3$ is $\simeq$60%, which is nicely consistent with the upper bound for PD_1 derived in Section 3. Finally, we note that in the framework of the above interpretation one may expect the other microflares in the source to be characterized by substantially lower polarization degrees and larger misalignments between the polarization vector and the jet position angle (when compared with the microflare analyzed here) due to the inevitable spread in the kinematic parameters Γ and θ of small-scale shocks developing within the outflow. A similar geometrical approach for the interpretation of flux and *PD* variability was adopted by Raiteri et al. (2012, 2013) while analyzing data from long-term WEBT observations to account for the correlation between flux and *PD* in blazar 4C 38.41 and the anti-correlation in BL Lacertae objects.

The above interpretation is obviously not unique, and several other models—including, for example, a helical distortion in strongly magnetized plasma subjected to MHD instabilities—may possibly account for the observational findings as well. Also, if the flaring zone consists of an underlying, highly uniform longitudinal magnetic field on top of which a shock propagates, injecting freshly accelerated particles, it is plausible that the observed $F-PD$ anti-correlation is due to a reduction in the net polarization by an increasing transverse field related to the shock compression of a random, small-scale magnetic field component (see in this context Cawthorne et al. 1993). Only a regular, multi-band photo-polarimetric monitoring of the source with a time resolution of the sub-hour scale, allowing for a more precise characterization of multiple optical microflares in S5 0716+714, could tighten modeling constraints and disprove various alternative scenarios, providing unique insight into the small-scale structure of relativistic outflows in AGNs in general. The robust conclusion from the analysis presented in this Letter, however, is that the small-amplitude flux changes observed in blazar sources are related to uniform, coherent emission regions characterized by a highly ordered magnetic field and small linear sizes of the order of $\ell \sim 10^{15}\,(\tau_{\rm var}/{\rm hr})\,(\delta/10)\,{\rm cm}$ and, as such, constitute (most likely) only small sub-volumes of the outflows.

The authors acknowledge support from the following grants and institutions: the Polish National Science Centre grants DEC-2012/04/A/ST9/00083 (G.B., A.G., M.O., Ł.S.) and 2013/09/B/ST9/ 00599 (S.Z.); National Natural Science Foundation of China grant 11203016 (S.-M.H.); the Russian

RFBR grants 15-02-00949 and 15-32-50887, and St. Petersburg University research grant 6.38.335.2015 (St. Petersburg University team); project FR/639/6-320/12 by the Shota Rustaveli National Science Foundation under contract 31/76 (Abastumani team); the observing grant support from the Institute of Astronomy and Rozhen National Astronomical Observatory, Bulgarian Academy of Sciences, and project Nos. 176011, 176004, and 176021 supported by the Ministry of Education, Science and Technological Development of the Republic of Serbia (G.D. and O.V.); NASA under Fermi Guest Investigator grant NNX14AQ58G (BU group). AZT-24 observations are made within an agreement between Pulkovo, Rome and Teramo observatories.

REFERENCES

Andruchow, I., Romero, G. E., & Cellone, S. A. 2005, A&A, 442, 97
Bach, U., Krichbaum, T. P., Ros, E., et al. 2005, A&A, 433, 815
Begelman, M. C., Blandford, R. D., & Rees, M. J. 1984, RvMP, 56, 255
Bevington, P. R., & Robinson, D. K. 2003, in Data Reduction and Error Analysis for the Physical Sciences, ed. R. B. Philip & D. R. Keith (3rd ed., Boston, MA: McGraw-Hill), 39
Bhatta, G., Webb, J. R., Hollingsworth, H., et al. 2013, A&A, 558, 92
Camenzind, M., & Krockenberger, M. 1992, A&A, 255, 59
Cawthorne, T. V., & Cobb, W. K. 1990, ApJ, 350, 536
Cawthorne, T. V., Wardle, J. F. C., Roberts, D. H., & Gabuzda, D. C. 1993, ApJ, 416, 519
Covino, S., Baglio, M. C., Foschini, L., et al. 2015, A&A, 578, A68
Fan, J.-H., Tao, J., Qian, B.-C., et al. 2011, RAA, 11, 1311
Goyal, A., Krishna, G. W., Paul, J., Stalin, C. S., & Sagar, R. 2013, MNRAS, 435, 1300
Hagen-Thorn, V. A., Larionov, V. M., Jorstad, S. G., et al. 2008, ApJ, 672, 40
Howell, S. B. 1989, PASP, 101, 616
Hu, S. M., Chen, X., Guo, D. F., Jiang, Y. G., & Li, K. 2014, MNRAS, 443, 2940
Hughes, P. A., Aller, H. D., & Aller, M. F. 1985, ApJ, 298, 301
Kollgaard, R. I., Wardle, J. F. C., & Roberts, D. H. 1990, AJ, 100, 1057
Laing, R. A. 1980, MNRAS, 193, 439
Laing, R. A. 2002, MNRAS, 329, 417
Larionov, V. M., Jorstad, S. G., Marscher, A. P., et al. 2013, ApJ, 768, 40
Lyutikov, M., Pariev, V. I., & Gabuzda, D. C. 2005, MNRAS, 360, 869
Marscher, A. P. 2014, ApJ, 780, 87
Meier, D. L. 2012, in Black Hole Astrophysics: The Engine Paradigm, ed. D. L. Meier (Berlin: Springer), 655
Morozova, D. A., Larionov, V. M., Troitsky, I. S., et al. 2014, AJ, 148, 42
Nalewajko, K. 2009, MNRAS, 395, 524
Narayan, R., & Piran, T. 2012, MNRAS, 420, 604
Perlman, E. S., Adams, S. C., Cara, M., et al. 2011, ApJ, 743, 119
Raiteri, C. M., Villata, M., D'Ammando, F., et al. 2013, MNRAS, 436, 1530
Raiteri, C. M., Villata, M., Smith, P. S., et al. 2012, A&A, 545, A48
Rani, B., Krichbaum, T. P., Marscher, A. P., et al. 2015, A&A, 578, A123
Rybicki, G. B., & Lightman, A. P. 1986, in Radiative Processes in Astrophysics, ed. G. B. Rybicki & A. P. Lightman (New York: Wiley), 400
Saito, S., Stawarz, Ł., Tanaka, Y. T., et al. 2015, ApJ, arXiv:1507.02442
Sakimoto, K., Uemura, M., Sasada, M., et al. 2013, PASJ, 65, 35
Sasada, M., Uemura, M., Arai, A., et al. 2008, PASJ, 60, L37
Sironi, L., Petropoulou, M., & Giannios, D. 2015, MNRAS, 450, 183
Subramanian, P., Shukla, A., & Becker, P. A. 2012, MNRAS, 423, 1707
Uemura, M., Kawabata, S., Sasada, M., et al. 2010, PASJ, 62, 69
Villforth, C., Nilsson, K., Østensen, R., et al. 2009, MNRAS, 397, 1893
Wagner, S. J., & Witzel, A. 1995, ARA&A, 33, 163
Wardle, J. F. C., Cawthorne, T. V., Roberts, D. H., & Brown, L. F. 1994, ApJ, 437, 122
Watson, D., Hanlon, L., McBreen, B., et al. 1999, A&A, 345, 414
Webb, J. R. 2007, BAAS, 39, 93
Webb, J. R., Howard, E., Benítez, E., et al. 2000, AJ, 120, 41
Wu, J., Dai, Y., Zhou, X., & Ma, J. 2014, JApA, 35, 315